BULLETIN OF THE POLISH ACADEMY OF SCIENCES
TECHNICAL SCIENCES, Vol. 72(6), 2024, Article number: e151379
DOI: 10.24425/bpasts.2024.151379

CIVIL ENGINEERING

Differential vibrating-wire strain gauge for concrete deformation measurements

Adam KANCIRUK and **Elżbieta MATUS***

Strata Mechanics Research Institute Polish Academy of Sciences, Poland

Abstract. The basic measuring element of vibrating-wire strain gauges is a steel piano wire, functioning in the elastic range. This element is constantly under tension. Therefore, its material gradually deforms permanently. This deformation causes its stress to relax. This relaxation results in measurement errors of the strain gauges. This error, as demonstrated by both in situ and laboratory tests, can reach values of even several percent of the strain gauge measuring range (FSR) over periods of 10 years. Therefore, a concept of a differential strain gauge was proposed, for the construction of which two measuring wires would be used. Changing the input value of the strain gauge, i.e. a displacement of one of its anchors in relation to the other one would cause one wire to lengthen while the other wire shortened identically. The measured displacement would be calculated based on the difference in the frequency of the wire vibrations. In this way, the influence of the simultaneous relaxation of the wires on the measurement result would be greatly reduced. Based on this concept, a prototype differential strain gauge for measuring concrete deformation was realized. In addition to two wires, it also contains two electromagnets, placed together with the wires in a common body-housing. After the strain gauge was assembled, its first tests were carried out under laboratory conditions.

Keywords: measurement of deformations and displacements; vibrating-wire measuring instruments; strain gauge.

1. INTRODUCTION

Mechanical elastic elements are widely used in the construction of measuring instruments [1]. For example, popular load cells, manufactured by many domestic and foreign companies, contain an elastic element in the form of a solid of revolution, properly glued with electro-resistance strain gauges [3]. Measured input quantity – load $\boldsymbol{F}$ is converted by the elastic element into its deformation ε, measurable by strain gauges. The σ-ε characteristic of the elastic element material is therefore decisive for the load cell quality. Still popular magnetoelectric indicating meters contain an Archimedean spiral spring which generates a torque balancing the torque of the meter winding through which the measured current flows [4]. The deflection of the winding and the indicating pointer connected to it is therefore dependent on the properties of the spring, and here also the quality of the meter is determined by the σ-ε characteristic of the material from which it was made, among others. In the case of the measuring instruments mentioned as an example, their elastic elements are only subjected to constant stress during the measuring periods. While the values of input quantities of these instruments are zero, the stress on both the load cell elastic element and the meter spring is equal to zero.

One of the types of electromechanical gauges of non-electrical quantities into an electric measurable signal is a gauge based on a vibrating wire (VW) concept. Its main elastic element is a piece of the so-called piano wire [5]. The input quantity measured by the gauge is directly or indirectly converted into the tension σ of the wire. Depending on the tension, the wire (after appropriate stimulation) vibrates at the frequency $\boldsymbol{f}$ according to the theoretically derived equation (1) [6]:

$$f = \frac{1}{2l}\sqrt{\frac{\sigma}{\gamma}}, \tag{1}$$

where f – wire vibration frequency [Hz], l – wire length [m], σ – wire tension [Pa], γ – density of the wire material [kg/m^3].

The experimentally measured frequency of string vibrations does not differ from the frequency determined according to equation (1) by more than a few percent. In the case of strain VW gauges, the deformation of the tested object usually differs from the strain of the wire, because the measurement base of the gauge does not have to be equal to the active part of the wire length. Usually, for technical reasons (wire clamps and anchors), it is slightly longer [6].

For the wire to vibrate, it must be under tension even when the input quantity measured by the gauge is equal to zero. This is its so-called initial tension. According to the author's experience [6] the VW gauge works optimally when its wire tension is within the range of 220–660 MPa, i.e. when its strain varies from 1000 μm/m to 3000 μm/m (for Young's modulus E of the wire material equal to 220 GPa). At tensions lower than 220 MPa, the wire generates too distorted signal, at higher than 660 MPa – the wire material shows too much creep causing at its constant strain too much relaxation.

The above-mentioned relaxation of the wire material is the cause of the relaxation error of the gauge. This is manifested by a slow change in the frequency of its output signal towards its lower values at an unchanged measured quantity. The rhe-

*e-mail: wlosinska@imgpan.pl

Manuscript submitted 2024-03-21, revised 2024-07-23, initially accepted for publication 2024-07-24, published in November 2024.

ological properties of the wire can therefore be illustrated by the so-called Zener model [7]. This problem has been known for much longer in musical instruments than in metrology. Each stringed musical instrument requires periodic tuning [8] including the piano, although its strings are stretched on a massive cast-iron frame.

The measurement error resulting from the relaxation of the wire depends on its tension. Figure 1 shows the results of a seven-day study of VW strain gauges, both manufactured by one of the worldwide companies (charts A and B) [9] and the author-made gauges (C, D, and E) [6]. The process of the temporary increase in the relative error of the strain measurement is similar for all instruments, although the design of the gauges is different. Namely, in the case of the author's gauges, the ends of the wire are fixed (via clamps and anchors) to the tested object, and its deformation forces the wire tension to change directly. On the other hand, in commercially produced gauges, object deformations are transferred to the wire by means of a coil spring extending the measuring range of the device. The spring, however, is also an element that manifests relaxation, hence the good logical and quantitative consistency of the graphs. According to the catalog data of these gauges, their long-term stability should not exceed 0.2% FSR [9].

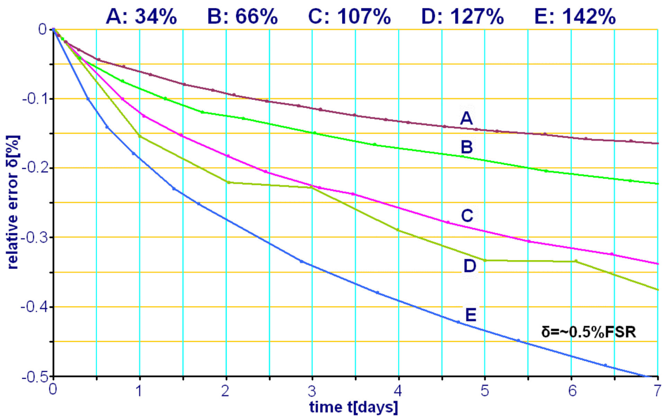

Fig. 1. Relative measurement errors resulting from the relaxation of 5 VW strain gauges depending on the stresses of their wires corresponding to the deformation measurements with values from 34% to 142% (still permissible) of the rated measuring range

The relaxation tests of a commercially produced gauge, without elements extending the measuring range, were also carried out (Fig. 2). The measurement results are presented in Figs. 3 and 4.

The gauge as shown in Fig. 2 is no longer produced and its technical data are not available. A gauge of a similar design [10]

Fig. 2. A VW strain gauge with the ends of the wire directly anchored to the tested object

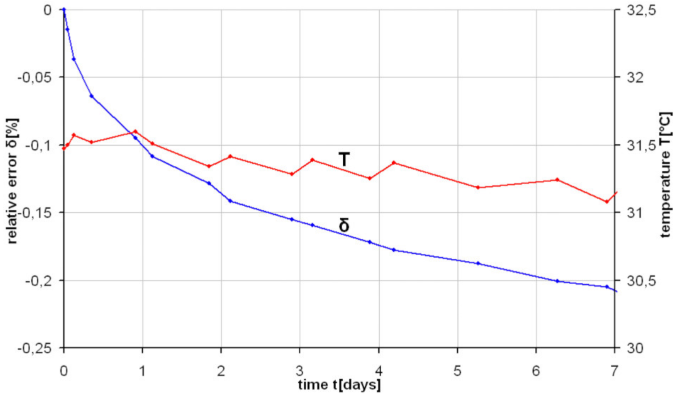

Fig. 3. Relative error of VW strain gauge relaxation (Fig. 2) after step application of deformation corresponding to a change in the tension of the wire by approx. 120% (still permissible) of the rated measuring range

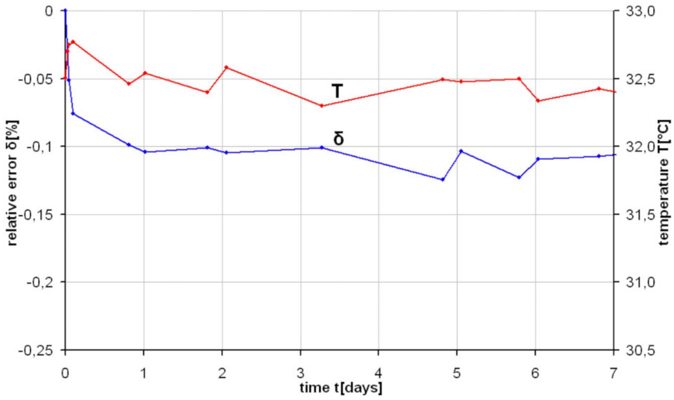

Fig. 4. Relative error of VW strain gauge relaxation (Fig. 2) after step application of deformation corresponding to a change in the tension of the wire by approx. 60% of the rated measuring range

shows a long-term zero stability equal to 0.02%/year. Its range is from 0 to 3000 μm/m. Stability at other points in the range is not reported. Another manufacturer of a very similar instrument determines its measurement stability in the same way [11].

As can be seen from the studies so far, the relaxation error of VW gauges is their inherent feature. The diagrams in Figs. 1, 3, and 4 are based on laboratory tests.

Since June 2011, the author has been measuring the deformation of the floor concrete slab of an airline hangar intended for servicing Airbus A320 passenger airplanes. For these measurements, delta rosettes [12], consisting of VW strain gauges with a base of 500 mm [6], were used. The rosettes were installed in the floor slab before the concrete hardened. These strain gauges, along with thermistor thermometers, were connected to automatic meter records, enabling periodic monitoring of deformation. Taking into account the above-mentioned test results, it is clear, that the measurements of the slab deformation must be affected by the relaxation error of the strain gauges.

The strain gauges measure both short-term deformations, caused by the pressure of the wheels of the serviced airplanes, and long-term deformations caused by the aging process of concrete in changing environmental conditions. Relaxation errors have a negligible impact on short-term deformations, as the service time of the airplanes rarely exceeds two days. Moreover, the values of these deformations only sporadically (once every few months from 2016) are in the range of 10–36 μm/m. It is related to cases of servicing larger airplanes than assumed. 10–36 μm/m corresponds to only 0.5–1.8% of the measuring range (FSR) of the used gauges (Fig. 5).

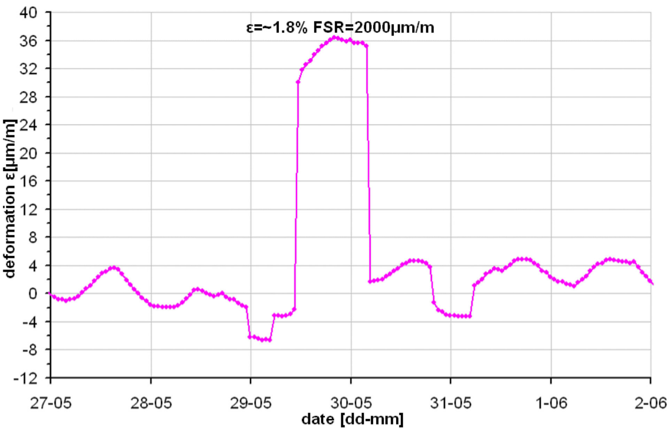

Fig. 5. The maximum operational deformation of the floor slab of the hangar recorded so far

On the other hand, the long-term strains are of the compressive type and reached approx. 360 μm/m. This corresponds to 18% of the measuring range of the gauges. This deformation, as mentioned, is among others a result of the slab concrete aging. Although the quoted value is typical for this process [13], it may contain a significant share of the false deformation resulting from the relaxation error of the strain gauges (Fig. 6).

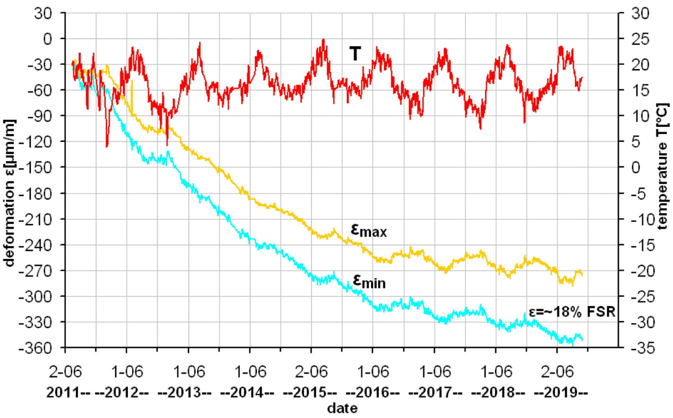

Fig. 6. Long-term main deformations (ε_{max} and ε_{min}) and temperature of the floor slab of the hangar

Many examples of the use of VW strain gauges for monitoring building structures are presented by manufacturers of VW apparatus on their websites in the 'Projects' or 'Applications' tabs [15]. The companies operating on the basis of the above-mentioned apparatus also do the same [17]. Nevertheless, monitoring of the deformation of building structures in areas affected by mining exploitation is usually carried out with the use of geodetic methods. For example, the article [18] describes the process of bending the southern wall of a residential building due to the deformation of its base ground. The authors placed a photograph of a fragment of a wall with a crack in Fig. 2 (page 215). Installing strain gauges in such locations, critical due to structural damage, can significantly enrich the overall measurement data collected during monitoring. In this way, strain gauge measurement methods become a significant supplement to the standard geodetic methods. Similarly, periodic inspection of the condition of buildings in mining areas is needed to determine the impact of ground deformation on the process of their gradual degradation [19]. In places particularly exposed to damage, this inspection may be conducted automatically with the use of the above-mentioned VW strain gauges. Such places are window openings, among others, and an example of the use of VW strain gauges in such places is given in [6]. Errors resulting from the relaxation of elastic elements of the strain gauges used should be as small as possible, or even negligible. Otherwise, the resulting false deformations (Fig. 1) will become comparable to the measured deformations, making the obtained measurement data unreliable. This is especially important in the case of deformation measurements of building structures built many years before starting the observation of their condition.

2. A CONCEPT OF MODIFICATION OF THE MECHANICAL SYSTEM OF THE STRAIN GAUGE FOR MEASURING CONCRETE DEFORMATION

The strain gauges for measuring concrete deformation, installed in its semi-liquid mixture before setting, have a very simple structure (Fig. 7). This applies to both commercially produced strain gauges and those constructed by the author [6].

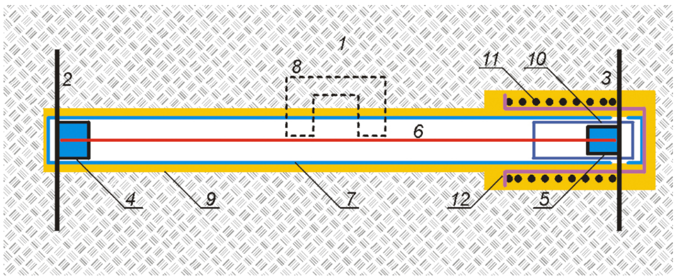

Fig. 7. A simplified scheme of the author's construction strain gauge for measuring the deformation of a concrete structure. *1* – concrete mass, *2*, *3* – anchors, *4*, *5* – wire clamps, *6* – wire, *7* – housing, *8* – electromagnet, *9* – flexible coating, *10* – sliding sleeve, *11* – pre-tension spring, *12* – yoke

Functioning of the strain gauge according to Fig. 7 is as follows. The deformation ε of the concrete mass *1* changes the distance between the anchors *2* and *3* Δl. As a result, the wire *6* is also deformed. This is accompanied by a change in its tension σ. The deformation of the wire is usually greater than the deformation of the concrete mass because the measuring base of the strain gauge – the distance between the anchors *2* and *3* is greater than the length of the active part of the wire *6*.

The role of electromagnet *8* is both to periodically stimulate wire *6* to vibrations and to convert these vibrations into sinusoidal alternating voltage. Its period $T = 1/f$ (equal to the period of the mechanical vibration of the wire) is measured by an external electronic meter. Due to the contraction of the concrete and the relaxation of the string material, this period increases. The wire is pre-tensioned by a coil spring *11*.

To compensate for the influence of the relaxation of the wire material on the result of concrete deformation measurement, at least partially, it is possible to extend the strain gauge according to the idea in Fig. 7 to a differential system. This system would include a double string and two electromagnets in a common mechanical system. The construction scheme of the proposed differential strain gauge is shown in Fig. 8.

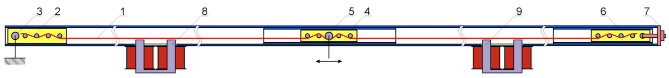

Fig. 8. Scheme of a differential strain gauge structure: *1* – wire, *2* –fixed wire clamp, *3* – fixed anchor, *4* – movable wire clamp, *5* – movable anchor, *6* – adjustable clamp, *7* – wire pre-tensioner, *8* and *9* – electromagnets

Mechanically, it is a combination of two strain gauges (let us sign them 'left' and 'right'), as shown in Fig. 7, functioning in an anti-parallel way. Therefore, for further consideration, it is easier to assume, that the device contains two wires: 'left' between the anchors *3* and *5*, and 'right' between the movable anchor *5* and the adjustable clamp *6*, although, in fact, it is one continuous piece of wire.

At rest position, the tension of the 'left' and 'right' wires is equal to σ_0. Concrete deformation changes the distance between anchors *3* and *5*, i.e. causes displacement of the anchor *5*. The clamp *6* is rigidly connected to the anchor *3* via the housing. In this way, moving the anchor *5* to the right will increase the tension to the value σ_1 of the 'left' wire and decrease the tension to the value σ_2 of the 'right' wire. Of course, when displacing the anchor 5 by Δl to the left, the stresses above the wires will change complementarily. The wires pre-tensioner is of the screw type, the pre-tension spring is unnecessary in this system.

For measurement results close to the middle of the gauge measuring range, the error resulting from the relaxation of the string material can be largely eliminated. From equation (1), the tension of the vibration wire can be determined:

$$\sigma = f^2 \cdot 4l^2\gamma. \tag{2}$$

The tension of the 'left' σ_1 and 'right' σ_2 strings is thus equal:

$$\sigma_1 = f_1^2 \cdot 4l^2\gamma, \qquad \sigma_2 = f_2^2 \cdot 4l^2\gamma. \tag{3}$$

The stresses σ_1 and σ_2 are the sum of the stresses resulting from the initial wire stress σ_0 minus the stress σ_R resulting from the relaxation of the wire material and the stress $\sigma_{\Delta l}$ resulting from the displacement of the anchor 5 (Fig. 8) by Δl:

$$\sigma_{\Delta l} = \frac{\Delta l}{l} E, \tag{4}$$

where l is the active length (between the clamps) of each wire, and E is Young's modulus. Thus, for the 'left' wire equation (2) has the form:

$$\sigma_0 - \sigma_R + \frac{\Delta l}{l} E = f_1^2 \cdot 4l^2\gamma, \tag{5}$$

and for the 'right' wire:

$$\sigma_0 - \sigma_R - \frac{\Delta l}{l} E = f_2^2 \cdot 4l^2\gamma. \tag{6}$$

After subtracting equations (5) and (6) by sides, we obtain:

$$2\frac{\Delta l}{l} E = \left(f_1^2 - f_2^2\right) \cdot 4l^2\gamma, \tag{7}$$

or

$$\Delta l = \left(f_1^2 - f_2^2\right) \cdot \frac{2l^3\gamma}{E}. \tag{8}$$

If the concrete deformation ε is to be determined from the displacement Δl, its value should be divided by the length of the strain gauge base equal to the distance between the anchors *3* and *5* (Fig. 8):

$$\varepsilon = \frac{\Delta l}{l_B} = \left(f_1^2 - f_2^2\right) \cdot \frac{2l^3\gamma}{E l_B}. \tag{9}$$

In equation (9), there is neither wire pre-stress σ_0 nor stress resulting from the relaxation of the wire material σ_R. This would suggest a complete compensation of the relaxation error for the measurement result value. This is theoretically the case only in the middle of the measuring range of the strain gauge. Any displacement Δl of the movable anchor beyond the neutral, middle position will result in a difference in the tension in the 'left' and 'right' wires. Bearing in mind that the relaxation rate of the wire depends on its tension (Fig. 1), it should be expected that the absolute relaxation error of the measurement results obtained with the differential strain gauge will depend on the value of these results alone. If tests of the prototype strain gauge show that this relationship is approximately linear, the relative relaxation error δ will have an approximately constant value over the entire measuring range. This is an uncommon feature of measuring instruments. Usually, the measurement error is determined in relation to their full-scale range (FSR). Therefore, the use of a small part of FSR (for example 10%) causes the results to be burdened with a significant relative error.

3. REALIZATION OF A PROTOTYPE DIFFERENTIAL VW STRAIN GAUGE

Figure 9 shows a prototype strain gauge made according to the idea presented in Fig. 6. Its measurement base (distance between anchors 2 and 3) is equal to 250 mm and the range is 2000 µm/m. The body, which is also the housing, is a stainless steel tube with a diameter of 12 mm. The wire clamps and anchors are made of structural steel, and the sliding sleeves are made of abrasion-resistant anodized aluminum [20]. The wires ('left' and 'right') have a diameter of 0.3 mm and an active length of 206 mm. Two double-coil electromagnets are mounted in such a way that the distance between their pole shoes and the wires is approx. 1 mm. They are also protected against damage with a housing made of duralumin and an epoxy compound. For installation in a semi-fluid concrete mix, the strain gauge needs to be covered with a flexible coating (except for the anchors) so that only the mentioned anchors are rigidly connected to the tested structure.

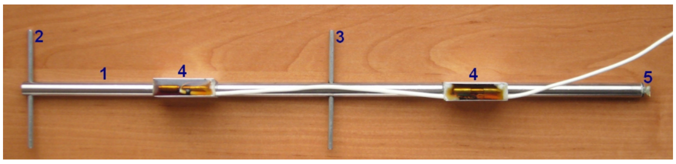

Fig. 9. Prototype differential VW strain gauge. *1* – body housing, *2* – fixed anchor, *3* – movable anchor, *4* – electromagnets, *5* – wire tensioner

4. STRAIN GAUGE RELAXATION TEST

In the first part of the test, the displacement of the movable anchor 3 (Fig. 9) was not forced externally, it occupied a neutral, middle position, determined by equally stretched (approx. 460 MPa) wires *1* (Fig. 8). The friction between the loose (~ 0.1 mm) and well-lubricated sleeve with clamp *4* (Fig. 8) and the body is negligible. To measure and record the results, a meter recorder was used, identical to that used in the hangar. The frequency of measurements was set at 400/24 hours. The wires were stretched approximately 30 minutes before the test, after which the strain gauge was placed in a temperature-stabilized chamber. To stabilize the temperature, a system with a contact thermometer with a threshold of 34°C, a simple electric circuit, and a heater were used. The two-state temperature stabilization system is always characterized by a hysteresis [21] in this case amounting to approximately 1°C. The thermal linear expansion coefficients of the strain gauge body (stainless steel) and the measuring wires (made of piano wire) are slightly different. Therefore, the hysteresis of temperature stabilization causes fluctuations in the wire stress and the results of the measurement of their vibration periods. This is clear in the following charts. However, these fluctuations do not interfere with the assessment of the tendency of changes in apparent wire deformations over almost eight days from the beginning of the test. The averaging approximation of the sequence of measurement results by the polynomial curve shows the relaxation of both wire stresses so that apparent deformations measured by both (‘left’ and ‘right’) component gauges exceed 30 μm/m (Fig. 10). Therefore the measurement error of the gauges with a range of 2000 μm/m each, would be greater than 1.5%. The applied differential system reduces the apparent strain gauge strain to less than 2 μm/m. Thus, its relaxation error decreases to less than 0.1% (Fig. 11).

To test the relaxation of the strain gauge at the displacement Δl of the movable anchor by about 75 μm, corresponding to concrete deformation of about 300 μm/m, the second part of the test was conducted. 300 μm/m corresponds to 15% of the measuring range of the gauge. To force the displacement of Δl, 2 massive adjustable yokes screwed to its anchors were used

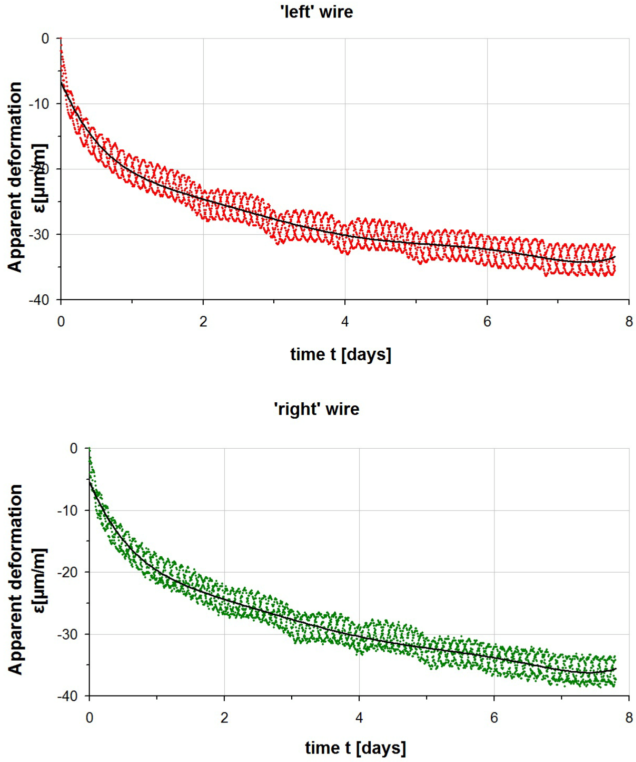

Fig. 10. The first part of the strain gauge test. Movable anchor in a neutral position, both wires stresses equal

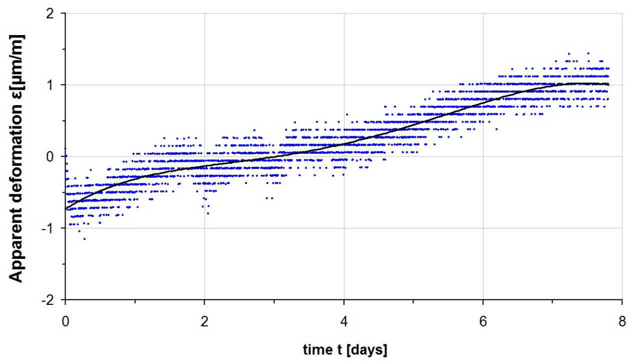

Fig. 11. Conditions as for Fig. 10, differential strain of the strain gauge and relaxation error

(Fig. 12). It was not possible to measure this displacement with an accuracy of better than 10%. At the present stage of research the properties of the strain gauge (its relaxation) this accuracy is not critical. This displacement was set in a stepwise manner, similar to the abrupt deformation of the hangar floor slab at the moment of entrance of the serviced airplane.

An interval of approximately 1 hour and 45 minutes was required between the two parts of the test. It was needed to put the mentioned yokes on the strain gauge, adjust them, place the system thus obtained into the above-mentioned chamber, and stabilize the temperature inside it. Thanks to the yokes, the ‘left’ gauge (Fig. 8) experienced an increase in tension by approx.

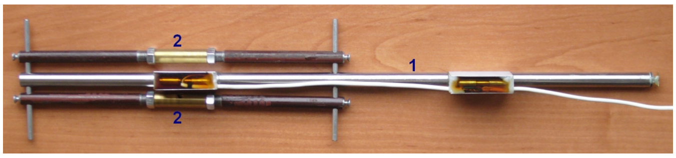

Fig. 12. The second part of the test. The movable anchor of the strain gauge 1 is connected to the fixed anchor by two adjustable yokes 2

15%, and the 'right' one – a similar decrease. The response of both component gauges is shown in Figs. 13 and 14. The false part of the strain measured by the gauge (derived from the relaxation of the wire) was significantly reduced due to its differential structure.

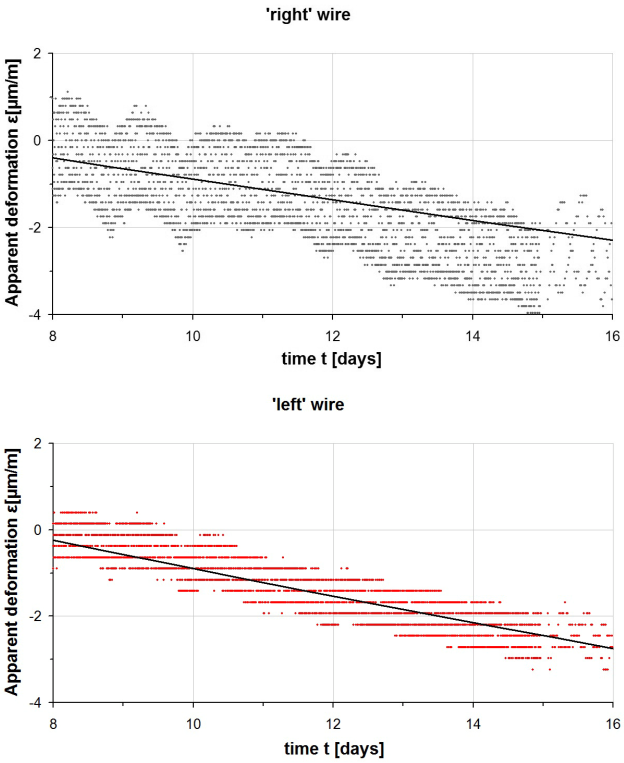

Fig. 13. The second part of the strain gauge test. Deformations measured by the component gauges and their relaxation errors

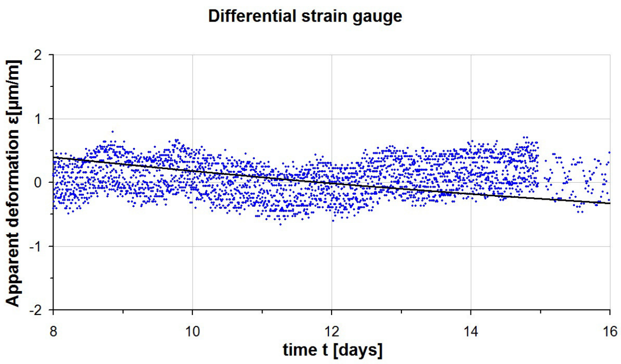

Fig. 14. Deformations measured by the differential gauge and its relaxation errors

Another feature of the piano wire, which is the memory effect, was revealed when the applied deformation was increased and, consequently, the right wire tension was decreased stepwise. This is shown in Fig. 15. After relaxation, the wire shows a short-term increase in stress. This behaviour is in line with the Zener rheological model. The differential strain gauge slightly reduces this effect, because the 'left' wire (more tensioned) – does not show this effect to the same extent (Fig. 16). It should be noted, however, that as significant as during the test step changes

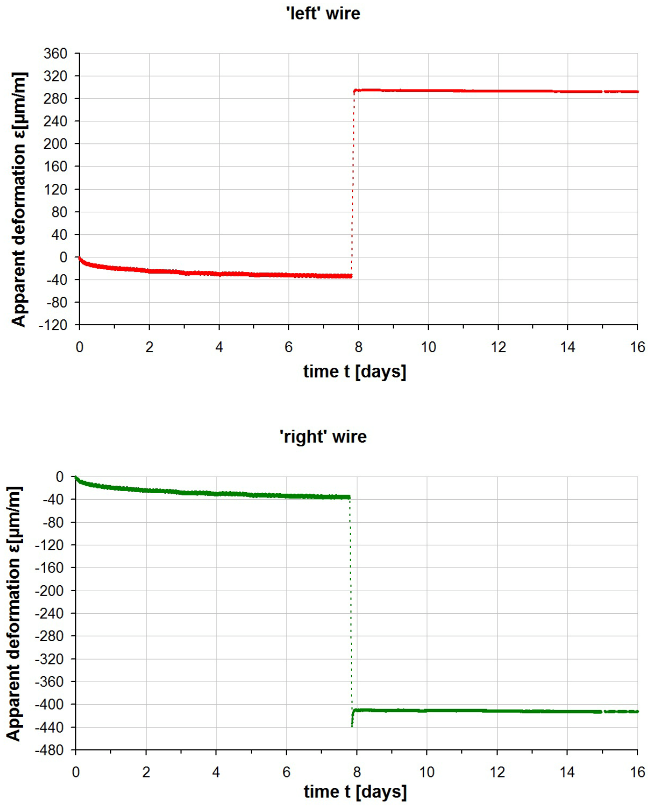

Fig. 15. Total deformations measured by both component gauges during both parts of the test. The arrow indicates the effect of the 'right' wire memory effect on the measurement results

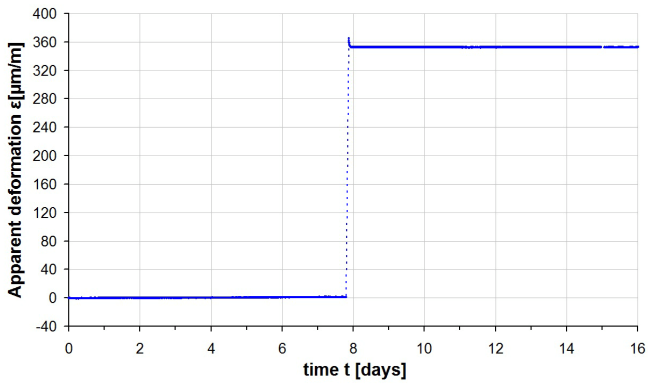

Fig. 16. Total deformations measured by the differential gauge during both parts of the test. The influence of the wire memory effect on the measurement results is slightly reduced

in applied deformation (~ 15% FSR of the gauge) are much greater than the maximum reached practicable (~ 1.8% FSR). Therefore, the influence of the considered memory effect on the measurement results of the deformation of the hangar floor slab may not be noticeable. This is evidenced by the results of measurements conducted so far (Fig. 5).

The disadvantage of the differential strain gauge compared to its 'single', simple form is the greater complexity of its structure, wiring, and larger dimensions. As usual, it is proposed to use this type of strain gauge in rosette systems (Fig. 17). This enables the determination of the flat deformation state of a concrete structure. The rosette consisting of differential strain gauges protrudes beyond the outline of the rosette consisting of 'single' strain gauges by more than 200 mm. Therefore, when choosing a place for its installation, its increased dimensions should be taken into account.

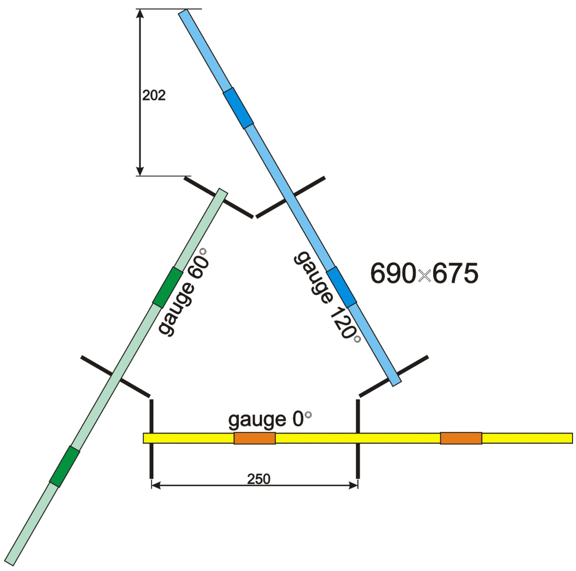

Fig. 17. Proposed arrangement of the rosette consisting of differential strain gauges and its overall dimensions

5. SUMMARY AND CONCLUSIONS

The first tests of the differential VW strain gauge show its significant advantages compared to 'single' ones. This applies to commercially manufactured gauges as well as those elaborated and used by the author. The author has not encountered a similar construction so far. The use of the differential system of two measuring wires significantly reduces errors resulting from their relaxation. This clearly improves the long-term metrological parameters of the gauge.

The design of the VW differential strain gauge is more complex than that of a 'simple' strain gauge but is simpler than that of two independent ones because it contains no spring system for pre-tensioning the wire. Stainless steel tubes were used as the body of the strain gauge instead of aluminum ones. This has the advantage of having a coefficient of thermal expansion which is closer to that of a piano wire. In addition, as a stiffer material, it provides much greater resistance to damage the gauge when installed in the semi-fluid concrete mix. Further research will be devoted to optimizing its parameters to obtain a transducer with appropriate metrological properties (e.g. temperature stability, time stability).

The next stage could be the construction of the rosette as above and applying it to in-situ research.

REFERENCES

[1] G. Cieplok, L. Bednarski, and R. Sieńko, "The application of self-excited wibrations for dynamic strain measurements carried out by vibrating wire tensometers," *Mech. Control*, vol. 34, no. 1, pp. 1–7, 2015, doi: 10.7494/mech.2015.34.1.1.

[2] S. Emmerik *et al.*, "Measuring Tree Properties and Responses Using Low-Cost Accelerometers," *Sensors*, vol. 17, no. 5, p. 1098, 2017, doi: 10.3390/s17051098.

[3] X. Wang, "Thermal strain measurement of EAST W/Cu divertor structure using electric resistance strain gauges," *Fusion Eng. Design*, vol. 113, pp. 1–5, 2016, doi: 10.1016/j.nme.2023.101483.

[4] J.-S. Chen and I.-S. Chen, "Deformation and vibration of a spiral spring," *Int. J. Solids Struct.*, vol. 64–65, pp. 166–175, 2015, doi: 10.1016/j.ijsolstr.2015.03.022.

[5] A. Borruto, G. Narducci, and M. Buccitti, "Failure analysis of piano strings," *Eng. Fail. Anal.*, vol. 35, no. 15, pp. 164–177, 2013, doi: 10.1016/j.engfailanal.2013.01.006.

[6] A. Kanciruk, *Metody tensometryczne w badaniach przemieszczeń, deformacji i zjawisk dynamicznych w gruncie i obiektach budowlanych*. Archives of Mining Sciences. Monograph 15, Kraków: Wydawnictwo Instytutu Mechaniki Górotworu PAN, 2012 (in Polish).

[7] Y. Gao, Q. Li, A. Dong, F. Wang, and X. Wang, "Characterizing the Resistance Relaxation of the Fabric-based Resistive Sensors Based on an Electro-mechanical Model," *Sens. Actuator A-Phys.*, vol. 310, no. 13, p. 112041, 2020, doi: I10.1016/j.sna.2020.112041.

[8] A. Szwajcowski and A. Pilch, "Optimization of piano tuning by means of spectral entropy minimization," *Appl. Acoust.*, vol. 166, p. 107359, 2020, doi: 10.1016/j.apacoust.2020.107359.

[9] Model 4420 Series, Vibrating Wire Crackmeter, Instruction Manual, Gekon. [Online]. Available: https://www.geokon.com/content/manuals/4420_Crackmeter.pdf (accessed: March 2024).

[10] Model 4000 Series, Vibrating Wire Strain Gauges, Instruction Manual, Gekon. [Online]. Available: https://www.geokon.com/content/manuals/4000_Strain_Gage.pdf (accessed: March 2024).

[11] Vibrating Wire Strain Gauge, RST Instruments Ltd. [Online]. Available: https://rstinstruments.com/wp-content/uploads/Vibrating-Wire-Strain-Gauge-ELB0007_24-1.pdf (accessed: March 2024).

[12] Z. Roliński, *Tensometria oporowa*. Warszawa: Wydawnictwo Naukowo-Techniczne, 1981 (in Polish).

[13] V. Gribniak, G. Kaklauskas, and D. Bacinskas, "Shrinkage in reinforced concrete structures: A computational aspect," *J. Civ. Eng. Manage.*, vol. 14, no. 1, pp. 49–60, 2008, doi: 10.3846/1392-3730.2008.14.49-60.

[14] M.H. Lai *et al.*, "Shrinkage design model of concrete incorporating wet packing density," *Constr. Build. Mater.*, vol. 280, no. 10, p. 122448, 2021, doi: 10.1016/j.conbuildmat.2021.122448.

[15] Gekon. [Online]. Available: https://www.geokon.com/ (accessed: March 2024).

[16] RST Instruments Ltd. [Online]. Available: https://rstinstruments.com/ (accessed: March 2024).

[17] NeoStrain Sp. z o.o. [Online]. Available: http://www.neostrain.pl/ (accessed: March 2024).

[18] L. Szojda and Ł. Kapusta, "Evaluation of the elastic model of a building on a curved mining ground based on the results of geodetic monitoring," *Arch. Min. Sci.*, vol. 65, no. 2, pp. 213–224, 2020, doi: 10.24425/ams.2020.133188.

[19] I. Bryt-Nitarska, "Studies of masonry structure technical wear in mining areas," *Arch. Min. Sci.*, vol. 64, no. 2, pp. 239–249, 2019, doi: 10.24425/ams.2019.128680.

[20] P. Totaro and B. Chusid, "Multistep anodization of 7075 – T6 aluminum alloy," *Surf. Coat. Technol.*, vol. 421, p. 127407, 2021, doi: 10.1016/j.surfcoat.2021.127407.

[21] J.M. Rahm, J. Löfgren, and P. Erhart, "Quantitative predictions of hermodynamic hysteresis: Temperature-dependent character of the phase transition in Pd–H," *Acta Mater.*, vol. 227, p. 117697, 2022, doi: 10.1016/j.actamat.2022.117697.